Disrupted topological properties of structural brain networks presents a glutamatergic neuropathophysiology in narcolepsy patients

Guoyan Chen[1†], Wen Wang[2†], Xiaopeng Kang[3†], Jiafeng Ren[1], Yingzhi Sun[2], Jun Zhang[1], Jiaxiu He[1], Shihui Sun[1], Zhao Zhong[1], Danqing Shang[1], Mengmeng Fan[1], Jinxiang Cheng[1], Xianchao Zhao[1], Jiaji Lin[1, 4*] and Changjun Su[1*]

1 Department of Neurology, The Second Affiliated Hospital of Air Force Medical University, No.569 Xinsi Road, Xi'an, 710038, China

2 Department of Radiology, The Second Affiliated Hospital of Air Force Medical University, No.569 Xinsi Road, Xi'an, 710038, China

3 School of Artificial Intelligence, University of Chinese Academy of Sciences, No.19A Yuquan Road, Beijing, 100876, China.

4 Department of Radiology, Chinese PLA General Hospital/Medical School of Chinese PLA, No.28 Fuxing Road, Beijing, 100853, China

[†]These authors contributed equally to this work.

*Correspondence to:

Jiaji Lin, Department of Neurology, The Second Affiliated Hospital of Air Force Medical University, No.569 Xinsi Road, Xi'an, 710038, China. Tel: 86-29-84777743 E-mail: jiaji90@outlook.com & Changjun Su, Department of Neurology, The Second Affiliated Hospital of Air Force Medical University, No.569 Xinsi Road, Xi'an, 710038, China. Tel: 86-29-84777744 E-mail: tdneurob@fmmu.edu.cn

Abstract (250 words)

Study objectives: Growing evidence have reported a number of abnormalities in the white matter bundles of narcolepsy patients. We sought to evaluate topological properties of brain structural networks, and their association with sleepiness and neuropathophysiological features in narcolepsy patients.

Methods: Diffusion tensor imaging (DTI) was conducted for 30 narcolepsy patients and matched healthy controls as well as sleepiness assessment and polysomnography. Structural connectivity for each patient was generated to analyze global and regional topological properties and their correlation with narcolepsy features. Further human brain transcriptome was extracted and spatially registered for connectivity vulnerability. Genetic functional enrichment analysis was performed and further clarified using *in vivo* emission computed tomography data.

Results: A wide and dramatic decrease in structural connetivities was observed in narcolepsy patients, with descending global network degree and global efficiency. These metrics were not only correlated with sleep latency and awakenning features, but also reflects alterations of sleep macrostructure in narcolepsy patients. Further network-based statistics identified a small hyperenhanced subnetwork of cingulate gyrus that is closely related to rapid eye movement sleep behavior disorder (RBD) in narcolepsy.

Conclusions: Narcolepsy patients endured a remarkable decrease in the structural architecture, which is not only be closely related to sleepiness symptoms but also glutamatergic signatures.

Keywords: narcolepsy; structural network; topological property; glutamatergic receptor; cingulate gyrus

Statement of Significance (120 words)

Growing evidence have identified a widespread disrupted white matter integrity of narcolepsy patients, so that connectome properties and neuropathophysiological features underlying these abnormalities have become a topic of increasing interest. This report extends on findings regarding the structural wirings and architectural topology of narcolepsy patients and inferring their clinical correlation with sleepiness assessment, polysomnography features and sleep macrostructure. Further imaging genetics analysis suggested glutamatergic signatures were responsible for the preferential vulnerability of connectivity alterations, while additional PET/SPECT data verified that structural alteration was significantly correlated with metabotropic glutamate receptor 5 (mGlutR5) and N-methyl-D-aspartate receptor (NMDA). Our findings, therefore, converge structural network and genetic signatures for in patients with narcolepsy.

Main text

1. Introduction

Narcolepsy is conceptualized as a state of instability or loss of boundary control that manifests as an inability to remain in sleep or wake states for the normal length of time and by the inappropriate occurrence of sleep phenomena during wakefulness, and vice versa [1]. Its onset peaks in the second decade of life and affects 1 in 2,000 people, and most people with narcolepsy also have symptoms indicative of cataplexy, sleep paralysis, hypnagogic hallucinations and disturbed nocturnal sleep [1]. A variety of neuroplastic alterations have been found to be closely associated with this wakefulness/sleep disturbances. Positron emission tomography (PET) study of Trotti et al. showed hypermetabolism in precuneus, inferior parietal lobule, superior and middle temporal gyri, and culmen [2]. In another study that used functional magnetic resonance imaging (fMRI), functional connectivity was decreased between regions of the limbic system and the default mode network (DMN), and increased in the visual network [3]. Furthermore, N-acetylaspartate/creatine-phosphocreatine in hypothalamus and myo-Inositol/ creatine-phosphocreatine in the amygdalain was reported to link with narcolepsy in 1H-MRS study of Joo et al [4]. Although disrupted brain functional activities have been widely reported in narcolepsy, the potential clinical implications of structural connectome abnormalities have not been systematically investigated.

The key attribute of the structural connectome is the large investment of neural resources in macroscale connectivity to keep the brain globally connected, with a considerable proportion of the anatomical communication pathways comprising white matter [5]. Cross-species studies on these wirings have revealed common “principles of network” appear to be widely conserved and represent fundamental features of brain organization and function [6]. Considerable effort in the past decade has been directed towards identifying network substrates and biomarkers that

predict disease severity, prognosis and outcome of specific brain disorders, such as deglobalization in the DMN / motor-core network in Alzheimer disease and ALS [7,8], fluctuation in functional network dynamics in epilepsy [9], hyperconnectivity in autism spectrum disorder [10], and so on. In recent years, growing evidences from Diffusion tensor imaging (DTI) have reported a number of abnormalities in the white matter bundles of narcolepsy patients. For example, Gool et al. have found brain-wide significantly lower fractional anisotropy (FA) in sleep-wake regulation-related, limbic and reward system areas of drug-free patients with narcolepsy type 1, which is sensitive to the fibers alignment and the myelination integrity [11]. Similar FA decreases have also been confirmed in the bilateral cerebellar hemispheres, bilateral thalami, corpus callosum and midbrain white matter of patients with narcolepsy type 2 [12,13]. Therefore, further analysis with network neuroscience tools may help us to discover topological features specific to this disease.

Therefore, current study obtained MR imaging from narcolepsy patients for structural connectome analysis. By characterizing alteration of global and regional signatures, we further associate them to clinical symptoms as well as underlying neuropathophysiological susceptibilities, which was further clarified by *in vivo* emission computed tomography data.

2. Materials and methods

2.1 Experiment design and participants

This is a prospective observational neuroimaging study aimed at exploring the clinical and brain imaging features of narcoleptic patients (ClinicalTrials.gov number, NCT03376568). It was approved by the Ethics Committee of the Second Affiliated Hospital (also named as Tangdu Hospital) of Air Force Medical University, and all patients and their families were fully informed and signed an informed consent form for the operation. From December 2017 to

December 2022, about 100 patients with narcolepsy were recruited at our out-patient narcolepsy clinic and signed up for the study. To be included, all subjects had to be 18-65 years old; right-handed according to the Edinburgh Handedness Scale [14] and have normal or corrected-to-normal vision. People with narcolepsy were diagnosed according to the 3rd edition of the International Classification of Sleep Disorders [15] and had to be treatment-naïve or off medication for ≥14 days prior to the study. The exclusion criteria included severe systematic diseases, central neurodegenerative diseases, cognitive impairment, unstable psychiatric diseases, structural brain abnormalities, history of intracranial hemorrhage or strokes, history of bleeding or coagulation abnormalities, inability to tolerate prolonged stationary position when supine, history of brain surgery, and contraindications for MRI scanning. MMSE and Beck's inventory were the tools used to initially screen for obvious mental illness and cognitive dysfunction before patient enrollment. Finally, a total of 30 patients with narcolepsy who met the criteria were included for multimodal MRI scanning. An additional 30 healthy controls (HCs) with matched gender and age were also enrolled at the same time and received the same MRI scanning as narcolepsy patients. All raw data are available on request within the conditions of our ethics approval.

2.2 Symptom assessment and imaging data acquisition

Patients and first-degree relatives underwent clinical consultations and semi-structured interviews about general characteristics (age, gender, previous medication use, excessive daytime sleepiness (EDS), cataplexy, sleep paralysis, hypnagogic hallucination, and rapid eye movement (REM) sleep behavior disorder (RBD)) as well as the Epworth Sleepiness Scale (ESS) (Johns, 1991) administered as a measure of daytime sleepiness. All data collection was performed during the afternoon and subjects were asked to refrain from caffeine containing substances for at least 24 h prior to examination. Clinical examinations including a neurological

examination have been performed with the multiple sleep latency test (MSLT) and polysomnography (PSG) as recommendation [16]. We ascertained a wide range of PSG parameters, including total sleep time, sleep efficiency with respect to both total registration and total sleep time, percentage of sleep stages N1, N2, N3, and REM (with respect to total sleep time), the latency to the first occurrence of these sleep stages from the beginning of the polysomnographic recording, wake time after sleep onset (WASO), awakenning number per hour (AWN), apnea-hypopnea index (AHI). Nocturnal rapid transitions from sleep onset into REM sleep (SOREMP) was defined as a latency of ≤15 minutes between sleep onset and the first epoch of REM sleep. Technicians awakened the patients after a registration time of roughly 7.5 hours.

MR images were acquired using a 3.0T MR imaging system (Discovery 750; GE Healthcare, Milwaukee, WI, USA) equipped with a 64-channel phase array coil. Both scanners were operated under quality control and assurance guidelines in accordance with the recommendations of the American College of Radiology and utilized the same imaging sequence. Participants were instructed to lie supine, relax, remain still, keep awake with eyes closed, and think of nothing during MRI acquisition. They wore ear plugs to reduce noise. To minimize head motion, tight but comfortable foam padding was placed around their heads.. The MRI scanning protocol included the following: (1) Diffusion tensor imaging (DTI): repetition time / echo time (TR / TE) = 7,522 / 80.8 ms; field of view (FOV) = 224 × 224; matrix = 112 × 112; b value = 1,000 sec/mm^2; encoding directions = 64; and B_0 = 4. (2) High-resolution sagittal 3D T1-weighted imaging (3D T1WI): TR / TE = 6.656 / 2.928 ms; inversion time = 800 ms; FA = 7°; FOV = 256 mm × 256 mm; matrix = 256 × 256; slice thickness = 1 mm; contiguous slices = 190). Two senior radiologists independently reviewed the aforementioned sequences, and carefully checked the quality of MRI images.

2.3 Network construction and subnetwork extract

DTI data were preprocessed using the DiffusionKit toolbox (http://diffusion.brainnetome.org) as previous report [17]. Briefly, the process included: (1) converting to DICOM data; (2) extracting a brain mask; (3) correcting for head motion and eddy current; (4) fitting diffusion tensors and performing tractography with a deterministic streamline method with the fractional anisotropy (FA) threshold of 0.3 and the angular threshold of 45°; (5) registering regions of interest (ROIs) from Montreal Neurological Institute (MNI) space to the individual space; (6) pruning tract for each ROI pair in the Brainnetome atlas (atlas.brainnetome.org) [18]. Brainnetome atlas includes middle frontal gyrus (MFG), parahippocampal gyrus (PhG), cingulate gyrus (CG), basal ganglia (BG) and other contralateral 24 partitions. The streamline number was referred to as connectivity by calculating for the tracts linking each pair of brain regions. All connectivity pairs were collected and then combined into 246 × 246 undirected and weighted connectivity matrix as global structural network. For ROI full names and abbreviations of the Brainnetome atlas, please refer to Supplementary Table 1.

Considering the regional variation in the structural subnetwork, network-based statistic was used to identify expansive disconnected subnetworks [19]. This non-parametric connectome-wide method is based on the principles underpinning traditional cluster-based thresholding of statistical parametric maps, and exploit the extent to which the connections comprising the contrast or effect of interest are interconnected [19]. Network-based statistics were performed with 5,000 permutations for weighted structural network comparisons between the narcoleptic patients and matched HCs. A threshold of $t = 3$ were applied for streamline comparison with a significance of $P < 0.05$ for permutation test.

2.4 Graph-Theory network analysis

We applied a sparsity threshold of 10% for the weighted network of each participant to avoid false connections. All graph-theory network analyses in this study were performed using the Brant toolbox (https://github.com/yongliulab/brant/) [20]. Topological metrics were calculated for each participant, reflecting different aspects of the structural network properties, including: (1) network / nodal degree is most commonly used as a measure of the wiring strength and coherence of anatomical network / ROI. The degree of an individual node not only reflects the cumulative "wiring cost" distribution of the regional network, but is also used as a measure of density distribution [21]. (2) global / nodal efficiency is measure of integration, which assessed parallel information transfer within a structural network / ROI. (3) clustering coefficient is measure of segregation, which is known as the fraction of triangles around an individual node, and the mean clustering coefficient for the network reflects, on average, the prevalence of clustered connectivity. For detailed calculation formulas and explanations on these metrics, we recommend Sporns' works [21-25].

2.5 Spatial alignment to neuropathophysiological features

We investigated the underlying neuropathophysiological features of narcolepsy patients using the human brain gene transcriptome data extracted from the Allen Human Brain Atlas (AHBA) [26]. This atlas is the first anatomically and genomically comprehensive three-dimensional human brain map, which contains a database of 20,737 gene expression levels represented by 58,692 probes. We matched the gene expression for each ROI to the Brainnetome atlas using the Abagen toolbox [27,28], by setting the threshold for intensity-based filtering of probes to 0.5. In the end, 236 ROI of 15, 633 genes were extracted, resulting in a 236 × 15,633 matrix for the alteration of nodal degree. One partial least squares (PLS) regression algorithm, the statistically inspired modification of the partial least squares (SIMPLS), was applied to investigate how genetic variance can explain brain structural

alterations [29]. The ranked gene list obtained using principle PLS weights was fed into the online tool WebGestalt [30] to identify the functional enrichment by gene set enrichment analysis (GSEA) [31]. The false discovery rate (FDR) correction was applied, along with a significance of $P < 0.05$ for all enrichment analyses. The entire workflow is shown in Supplementary Figure 1.

To further elucidate our GSEA results, we also introduced PET/SPECT maps of glutamatergic neuropathophysiological features from unrelated control groups for spatial alignment, which were collected by Justine et al [32]. Specifically, the [^{11}C]ABP688 data for the group I metabotropic glutamate receptor 5 (mGluR5) expression came from Rosa-Neto team, Dubois team and Smart team, respectively, while [^{18}F]GE-179 data for the ionotropic N-methyl-D-aspartate receptor (NMDA) expression came from Galovic's work. The correlation was calculated between the effect sizes of the ROI *t*-values and regional sum PET/SPECT values, resulting in a single measure for accessing the relationship between the altered brain structure and the glutamatergic features. To avoid false-positive results of spatial autocorrelation (SA), we generate 5,000 SA-preserving surrogate maps as null models using brainSMASH [33]. For the correlation analysis, we generated 5,000 SA preserving surrogate maps for each pattern as null models. The significance is calculated as $P_{Corr_SA} = \frac{Count_{Greater}}{Count_{All}}$, where $Count_{Greater}$ is the number that surrogate's absolute correlation coefficient is greater than that of the primary analysis. $Count_{All}$ are the times that performed surrogate correlation, in this case, 5,000 times.

2.6 Statistical Analysis and code availability

Chi-square tests were used to detect group differences between narcolepsy patients and matched HCs in the demographic analysis. Non-paired *t*-tests were used evaluate the difference in each connectivity between narcolepsy and matched HCs, as well as graph metrics

comparisons between narcolepsy and HCs or subgroup comparisons within narcolepsy patients. As for their clinical relevance, Pearson's correlation coefficient serves as a measure. The level of significance was set at $P < 0.05$. Moreover, predictive performance of network degree was also evaluated for MSLT sleep latency by stepwise linear models with leave-one-out cross-validation (LOOSWR). Network degree were fit into linear regression with adjustment of subject's sex, age, and constant. Using both forward and backward iterations (entered a model), iterations with a significance < 0.05 were count and its proportion is analyzed. Predicted MSLT sleep latency were compared using Pearson correlation coefficients too. Majority of the computations were performed in the Python engine. All the statistical process and analysis code are available at https://github.com/Jiaji-Lab.

3. Results

3.1 Demographic characteristics of patients with narcolepsy

The data of 30 narcolepsy patients (Male: Female = 18: 12) were finally collected with mean age (± SD) of 29.5 ± 13.5 years. Compared with HCs, all patients explicitly complaint of EDS with a mean duration of 10.0 ± 7.0 years, of which 56.67% patients (17/30) had cataplexy, 20.00% patients (6/30) had sleep paralysis, 40.00% patients (12/30) had hypnagogic hallucinations, and 63.33% patients (19/30) had RBD, respectively. These narcolepsy patients had significantly higher ESS score than matched health controls (15.4 ±5.2 *vs.* 2.8 ± 2.0, $P < 0.001$) as well as low MSLT sleep latency of 2.25 ± 1.39 min with ≥ 2 sleep-onset REM episodes. Brain MRI revealed no gross abnormalities in any patients with narcolepsy. Diagnostic overnight PSG examination was performed for all of them. Detail demographic characteristics and PSG characteristics are summarized in Table 1.

3.2 Topology features of structural network in patients with narcolepsy

To study the alterations in brain structural network of narcolepsy patients, all the structural connectivities of each patient were constructed. Non-paired *t*-test for each structural connectivity was calculated between narcolepsy patients and matched HCs, and all *t*-values were collected for global contrast matrix and converted into *t*-values distribution (Fig. 1A). As *t*-values distribution shown, a wide range of structural connectivities were found to endure a remarkable decrease without FDR correction in patients with narcolepsy compared with matched HCs, as well as a small fraction of enhanced connectivities (Fig. 1B). The most significant decreased structural connectivity were right ventrolateral area 6 (A6vl_R) of MFG to right inferior frontal junction (IFJ_R) of MFG (t = -5.594, n = 30), left caudal hippocampus (cHipp_L) to left caudal temporal thalamus (cTtha_L) (t = -5.481, n = 30), and left rostral area 35/36 (A35/36r_L) of PhG to cHipp_L (t = -5.328, n = 30).

Graph metrics of global structural network were calculated and a significant decrease in the network degree in narcolepsy patients were observed compared to matched HCs (P < 0.001) as well as integration measure of global efficiency (P < 0.001, Fig. 1C). There was no significant difference in the segregation measure of clustering coefficient between narcolepsy and HCs group (Fig. 1C). We further compared subgroups of narcolepsy patients with according to the clinical characteristics (cataplexy, sleep paralysis, hypnagogic hallucination and RBD), and no significant difference between subgroups was found. After FDR correction of all ROIs, nodal degree of 33 ROIs and nodal efficiency of 150 ROIs were found endured significant declines (Fig. 1D).

As for small but significant positive peak in *t*-values distribution of contrast matrix, we tried network-based statistics to better identify the hyperenhanced subnetwork. The analysis revealed a small subnetwork within 7 ROIs (P < 0.001), including both sides of caudal area

23 (A23c_L and A23c_R) of CG, right ventral caudate (vCa_R), globus pallidus (GP_R) and dorsal caudate (dCa_R) of BG, and left medial pre-frontal thalamus (mPFtha_L) and rostral temporal thalamus (rTtha_L) of Tha (Fig. 1E). Graph metrics of this subnetwork were not only found increased in the narcolepsy patients (network degree: $P < 0.001$; global efficiency: $P < 0.001$, Fig. 1F), but also significantly increased in the narcolepsy patients with RBD *vs.* without RBD (network degree: $P < 0.05$; global efficiency: $P < 0.05$; Fig. 1F). So that it is referred to as the RBD-sensitive subnetwork.

3.3 Linking structural topology to clinical characteristics of narcolepsy patients

We analyzed the correlation between graph metrics and clinical characteristics within narcolepsy patients. There was no significant correlation between graph metrics and gender or age. Although neither network degree nor global efficiency was correlated with ESS score of narcolepsy patients, it turns out that both network degree and global efficiency were positively correlated with MSLT sleep latency (network degree: $r = 0.59$, $P < 0.001$; global efficiency: $r = 0.55$, $P = 0.002$; Fig.2A). Similarly, they were also positively correlated with sleep latency at night PSG (network degree: $r = 0.54$, $P = 0.002$; global efficiency: $r = 0.51$, $P = 0.004$; Fig.2A). Moreover, they endured a significant negative correlation with WASO (network degree: $r = -0.45$, $P = 0.013$; global efficiency: $r = -0.45$, $P = 0.012$) and AWN (network degree: $r = -0.38$, $P = 0.039$; Fig.2B). As for sleep macrostructure, global efficiency but not network degree was negatively correlated with the N1 sleep time ($r = -0.36$, $P = 0.047$) and percentage ($r = 0.37$, $P = 0.043$; Fig.2C). Not only the network degree was positively correlated with the N2 sleep time ($r = 0.44$, $P = 0.015$) and percentage ($r = 0.38$, $P = 0.037$), but also the network global efficiency was significantly correlated (the N2 sleep time: $r = 0.51$, $P = 0.004$; N2 sleep percentage: $r = 0.46$, $P = 0.009$; Fig.2C). No metrics was found correlated with N3 or REM

sleep or other clinical characteristics. Finally, we also studied the graph metrics of RBD-sensitive subnetwork, and it only has significant correlation with RBD symptoms (spearman r = -0.76, P = 0.0178). No other significant correlation was found for RBD-sensitive subnetwork within narcolepsy patients.

As remarkable correlation with MSLT sleep latency ($P_{FDR} < 0.05$), network degree was also applied in LOOSWR for MSLT Sleep latency prediction with adjustment of gender and age. It was found that network degree could be used as reliable biomarkers for MSLT sleep latency prediction (r = 0.71; iterative repetition = 100%, $P_{FDR} < 0.05$).

3.4 Linking structural narcolepsy topology to glutamatergic neuropathophysiology

We performed a PLS-based gene analysis to identify genes that were highly correlated with alterations of structural network in patients with narcolepsy. Gene expression networks of both hemispheres of the healthy adult brain were constructed using the AHBA [34]. The primary PLS features of narcolepsy genes accounted for 21.19% of the total variance with the $P < 0.001$ based on 5,000 permutations. These rank-list of narcolepsy-featured genes were annotated, and the Panther pathway analysis identified that these featured genes were functionally enriched in Metabotropic glutamate receptor (mGlutR) group I pathway (P00041, $P_{FDR} < 0.001$), Ionotropic glutamate receptor (iGlutR) pathway (P00037, $P_{FDR} < 0.001$) and Interferon-gamma (IFNγ) signaling pathway (P00035, $P_{FDR} < 0.001$; Fig. 3A). We then further investigate their GO characteristics. A post-processing step of affinity propagation revealed that the representative biological processes of the narcolepsy-featured genes were synaptic vesicle cycle (GO0099504), regulation of synapse structure or activity (GO:0050803), glutamate receptor signaling pathway (GO0007215) and regulation of membrane potential (GO0042391) (all $P_{FDR} < 0.001$; Fig. 3B). Majority of cellular components focused on synaptic membrane

(GO: 0097060) and glutamatergic synapse (GO:0098978) (all $P_{FDR} < 0.001$; Fig. 3B). All the top gene functional properties are provided in Supplementary Tables 2-4.

As glutamatergic neuropathophysiology had the highest significance in functional analysis, we tried further verification by glutamatergic PET/SPECT data from unrelated healthy subjects. With 5,000 SA-preserving surrogate maps as null models, there were significant correlations between the global network degree and mGluR5 (r = -0.37, -0.38 and -0.35 respectively for Rosa-Neto, Dubois and Smart data, all $P < 0.001$; Fig. 3C) and NMDA (r = -0.34 for Galovic data, $P < 0.001$; Fig. 3D).

4. Discussion

In our present study, we explored the abnormal alteration in the overall structural network in narcolepsy patients, revealing a wide and significant wiring decline. It not only suggested a dramatic decrease in the global efficiency of the structural connectivity, but also showed a significant clinical correlation with sleep latency, nocturnal awakening, and sleep macrostructure. It also showed that this structural alteration was closely linked to functional signature of glutamatergic neuropathophysiology, which was further confirmed by *in vivo* emission computed tomography data of mGluR5 and NMDA. All these suggest that we need to pay more attention to the neuroplasticity features of the brain connectome adaptation in narcolepsy.

The human brain is a complex computational system which was widely connected by network of “highways” the information flow along. With the improvement of non-invasive imaging systems and their increasing resolution, much efforts toward investigating brain connectome focuses on the application of graph theoretical analysis, which facilitate explorations of the information propagation, integration, and segregation that characterize the

topology of the network [35]. It was widely reported in various neurological diseases, such as dementia, multiple sclerosis and stroke, that a bunch of architectural features were found sensitive to early disease diagnosis and symptom assessment, including small-worldness [36], efficiency [37], modularity [38], network hubs [39], and rich-club organization [40]. In recent years, alteration in connectome have been found to be also sensitive to functional disorders such as sleep disorders. For example, patients with insomnia disorder present a hyperconnectivity subnetwork related to right angular gyrus which contributes to increased reactivity and vulnerability [41]; obstructive sleep apnea makes patients more prone to connectivity dysfunction in the key nodes of the executive and default-mode networks [42]. In our current study, the alteration in structural properties of narcolepsy patients showed a close association with various symptoms (MLST sleep latency, awakening at night PSG and sleep macrostructure), emphasizing the potential value of further exploring the connectome features of this sleep disorder.

Another central question is that of the role that structural connectivity plays in shaping the brain activity dynamics of narcolepsy patients. Tremendous efforts in the early theoretical simulations relating structural and functional connectivity highlighted that anatomical variability is one of the major factors that promotes individualized static brain activity [43,44]. And modelling functional connectivity is not only use of brain structural connectivity data of a healthy brain but also increasingly need for that of brain disease [45,46]. In the study of narcolepsy, adolescent narcolepsy patients exhibited disrupted small-world network properties in functional activity as well as regional alterations in the caudate nucleus and posterior cingulate gyrus [3]. The abnormal connectivity between the hypothalamus and brain regions involved in memory consolidation during sleep, such as the hippocampus, may be linked to the loss of orexin containing neurons in the dorsolateral hypothalamus [47]. Further understanding the spatial properties, temporal dynamics, and spectral features of brain activity dynamics in

narcolepsy ask for study deeper characteristics of the structural connectivity itself as well as structure-function relationship research.

Although overall narcolepsy patients showed a significant decline in structural networks, it also highlighted an anomalously enhanced subnetwork involving the thalamus, striatum, and CG that was shown to be closely associated with RBD symptoms. RBD is characterized by a loss of REM sleep muscle atonia (RSWA) together with prominent motor behavioral manifestations associated with dreaming during REM sleep [48]. The frequency of RBD in narcolepsy with cataplexy seems to be fairly high, clinically evident in 45-61% and polysomnographically detectable in 36-43% of them [49]. However, these RBD of narcolepsy are quite far from idiopathic RBD in clinical phenotypes and consequences. They present less violent behaviors, fewer clinically relevant episodes, different sex ratio (affecting mostly men in the idiopathic form) and much earlier age at onset [50-52]. RBD may be an early symptom in narcolepsy childhood and preceded in severity and frequency with the aging process [53], but there is currently no indication that narcolepsy patients with RBD develop symptoms or signs of neurodegenerative disorders as idiopathic RBD did [54]. Moreover, due to the Braak hypothesis of Parkinson's Disease, tremendous studies of neural circuit mechanism on idiopathic RBD mainly focus on the brainstem destruction (especially in sublaterodorsal tegmental nucleus) [55,56], which was confirmed rarely existing in narcolepsy patients [57]. Therefore, it is necessary for us to further study the circuit mechanism within RBD-sensitive subnetwork of narcolepsy patients.

The difference between narcolepsy RBD and idiopathic RBD is also reflected in the significant difference in their neuropathophysiology mechanisms. Dopaminergic deficiency, shown by many studies using with SPECT/PET, is the most consistent neurochemical feature of idiopathic RBD [58]. However, in the study of narcolepsy, researchers are highly focused about the biological driving force of highly selective and severe loss of the hypocretinergic neurons

[59]. On one hand, various studies have shown that the activity of hypocretin is mediated by glutamate.When hypocretinergic neurons release hypocretin, the neurotransmitter attaches to glutaminergic receptor and induce a positive feedback of following hypocretin release [60,61]. On the other hand, hypothalamic secretin requires glutamate to perform its excitatory effects. It was reported that hypocretinergic neurons mainly released glutamate, and its effects may synergize with the excitatory effects of hypocretin [62,63]. When glutamate receptors are blocked, hypocretin does not exert its excitatory effect on motor neurons [62,63]. Hypocretinergic neurons also secrete neuronal activity-regulated pentraxin (NARP), a protein that promotes clustering of glutamatergic receptors at excitatory synapses and enhance postsynaptic responses to glutamate [64,65]. In our study, we found that glutamatergic neuropathophysiology may be a key factor that promote the form and extent of the narcolepsy brain remodeling circuits through connectomes, it worth further consideration of the protective treatment by glutamate blockable for narcolepsy.

Several methodological considerations should be contemplated when interpreting the results of this study. Our findings are based on structural data determined using diffusion tractography. The limitations of this method include the uncertainty of crossing fibers. There would be an improvement if high-angular resolution diffusion-weighted imaging or spherical deconvolution post-processing techniques are used to provide the best possible estimate of the underlying structural connectivity [66]. Using transcriptome and PET/SPECT data from healthy human brains could be limited if the narcolepsy gene expression patterns are different from those of healthy brains.

5. Acknowledgments

This work has been supported by the Key R&D Program of Shaanxi Province (Grant no. 2022ZDLSF03-07).

6. Conflict of Interest

The authors declare that they have no competing interests.

7. Disclosure Statement

Financial Disclosure: none. Non-financial Disclosure: none.

8. References

1. Bassetti CLA, Adamantidis A, Burdakov D, et al. Narcolepsy - clinical spectrum, aetiopathophysiology, diagnosis and treatment. Nature reviews Neurology. 2019; 15 (9): 519-539.

2. Trotti LM, Saini P, Crosson B, Meltzer CC, Rye DB, Nye JA. Regional brain metabolism differs between narcolepsy type 1 and idiopathic hypersomnia. Sleep. 2021; 44 (8).

3. Fulong X, Spruyt K, Chao L, Dianjiang Z, Jun Z, Fang H. Resting-state brain network topological properties and the correlation with neuropsychological assessment in adolescent narcolepsy. Sleep. 2020; 43 (8).

4. Poryazova R, Schnepf B, Werth E, et al. Evidence for metabolic hypothalamo-amygdala dysfunction in narcolepsy. Sleep. 2009; 32 (5): 607-613.

5. van den Heuvel MP, Sporns O. A cross-disorder connectome landscape of brain dysconnectivity. Nature reviews Neuroscience. 2019; 20 (7): 435-446.

6. van den Heuvel MP, Bullmore ET, Sporns O. Comparative Connectomics. Trends in cognitive sciences. 2016; 20 (5): 345-361.

7. Buckner RL, Sepulcre J, Talukdar T, et al. Cortical hubs revealed by intrinsic functional connectivity: mapping, assessment of stability, and relation to Alzheimer's disease. The Journal of neuroscience : the official journal of the Society for Neuroscience. 2009; 29 (6): 1860-1873.

8. Verstraete E, Veldink JH, van den Berg LH, van den Heuvel MP. Structural brain network imaging shows expanding disconnection of the motor system in amyotrophic lateral sclerosis. Human brain mapping. 2014; 35 (4): 1351-1361.

9. Pedersen M, Omidvarnia A, Curwood EK, Walz JM, Rayner G, Jackson GD. The dynamics of functional connectivity in neocortical focal epilepsy. NeuroImage Clinical. 2017; 15: 209-214.

10. Uddin LQ, Supekar K, Menon V. Reconceptualizing functional brain connectivity in autism from a developmental perspective. Frontiers in human neuroscience. 2013; 7: 458.

11. Gool JK, Fronczek R, Leemans A, Kies DA, Lammers GJ, Van der Werf YD. Widespread white matter connectivity abnormalities in narcolepsy type 1: A diffusion tensor imaging study. NeuroImage Clinical. 2019; 24: 101963.

12. Tezer FI, Erdal A, Gumusyayla S, Has AC, Gocmen R, Oguz KK. Differences in diffusion tensor imaging changes between narcolepsy with and without cataplexy. Sleep medicine. 2018; 52: 128-133.

13. Park YK, Kwon OH, Joo EY, et al. White matter alterations in narcolepsy patients with cataplexy: tract-based spatial statistics. Journal of sleep research. 2016; 25 (2): 181-189.

14. Oldfield RC. The assessment and analysis of handedness: the Edinburgh inventory. Neuropsychologia. 1971; 9 (1): 97-113.

15. Sateia MJ. International classification of sleep disorders-third edition: highlights and modifications. Chest. 2014; 146 (5): 1387-1394.

16. Krahn LE, Arand DL, Avidan AY, et al. Recommended protocols for the Multiple Sleep Latency Test and Maintenance of Wakefulness Test in adults: guidance from the American Academy of Sleep Medicine. Journal of clinical sleep medicine : JCSM : official publication of the American Academy of Sleep Medicine. 2021; 17 (12): 2489-2498.

17. Lin J, Kang X, Xiong Y, et al. Convergent structural network and gene signatures for MRgFUS thalamotomy in patients with Parkinson's disease. NeuroImage. 2021; 243: 118550.

18. Yu C, Zhou Y, Liu Y, et al. Functional segregation of the human cingulate cortex is confirmed by functional connectivity based neuroanatomical parcellation. NeuroImage. 2011; 54 (4): 2571-2581.

19. Zalesky A, Fornito A, Bullmore ETJN. Network-based statistic: identifying differences in brain networks. 2010; 53 (4): 1197-1207.

20. Xu K, Liu Y, Zhan Y, Ren J, Jiang T. BRANT: a versatile and extendable resting-state fMRI toolkit. Frontiers in neuroinformatics. 2018; 12: 52.

21. Rubinov M, Sporns OJN. Complex network measures of brain connectivity: uses and interpretations. 2010; 52 (3): 1059-1069.

22. Barthelemy MJTEpjB. Betweenness centrality in large complex networks. 2004; 38 (2): 163-168.

23. Smith P, Hutchison D, Sterbenz JP, et al. Network resilience: a systematic approach. 2011; 49 (7): 88-97.

24. Phillips C, Swiler LP. A graph-based system for network-vulnerability analysis. In: proceedings from the Proceedings of the 1998 workshop on New security paradigms; 1998.

25. Najjar W, Gaudiot J-LJIToC. Network resilience: A measure of network fault tolerance. 1990; 39 (2): 174-181.

26. Hawrylycz MJ, Lein ES, Guillozet-Bongaarts AL, et al. An anatomically comprehensive atlas of the adult human brain transcriptome. Nature. 2012; 489 (7416): 391-399.

27. *abagen: A toolbox for the Allen Brain Atlas genetics data* [computer program]. 2020.

28. Arnatkeviciute A, Fulcher BD, Fornito A. A practical guide to linking brain-wide gene expression and neuroimaging data. Neuroimage. 2019; 189: 353-367.

29. Seidlitz J, Vasa F, Shinn M, et al. Morphometric Similarity Networks Detect Microscale Cortical Organization and Predict Inter-Individual Cognitive Variation. Neuron. 2018; 97 (1): 231-247 e237.

30. Liao Y, Wang J, Jaehnig EJ, Shi Z, Zhang B. WebGestalt 2019: gene set analysis toolkit with revamped UIs and APIs. Nucleic Acids Res. 2019; 47 (W1): W199-W205.

31. Subramanian A, Tamayo P, Mootha VK, et al. Gene set enrichment analysis: a knowledge-based approach for interpreting genome-wide expression profiles. Proc Natl Acad Sci U S A. 2005; 102 (43): 15545-15550.

32. Hansen JY, Shafiei G, Markello RD, et al. Mapping neurotransmitter systems to the structural and functional organization of the human neocortex. Nature neuroscience. 2022; 25 (11): 1569-1581.

33. Burt JB, Helmer M, Shinn M, Anticevic A, Murray JD. Generative modeling of brain maps with spatial autocorrelation. Neuroimage. 2020; 220: 117038.

34. Hawrylycz M, Miller JA, Menon V, et al. Canonical genetic signatures of the adult human brain. 2015; 18 (12): 1832.

35. Rubinov M, Sporns O. Complex network measures of brain connectivity: uses and interpretations. NeuroImage. 2010; 52 (3): 1059-1069.

36. Sporns O, Chialvo DR, Kaiser M, Hilgetag CC. Organization, development and function of complex brain networks. Trends in cognitive sciences. 2004; 8 (9): 418-425.

37. Latora V, Marchiori M. Efficient behavior of small-world networks. Physical review letters. 2001; 87 (19): 198701.

38. Sporns O, Betzel RF. Modular Brain Networks. Annual review of psychology. 2016; 67: 613-640.

39. van den Heuvel MP, Sporns O. Network hubs in the human brain. Trends in cognitive sciences. 2013; 17 (12): 683-696.

40. van den Heuvel MP, Sporns O. Rich-club organization of the human connectome. The Journal of neuroscience : the official journal of the Society for Neuroscience. 2011; 31 (44): 15775-15786.

41. Wei Y, Bresser T, Wassing R, Stoffers D, Van Someren EJW, Foster-Dingley JC. Brain structural connectivity network alterations in insomnia disorder reveal a central role of the right angular gyrus. NeuroImage Clinical. 2019; 24: 102019.

42. Canessa N, Castronovo V, Cappa SF, et al. Sleep apnea: Altered brain connectivity underlying a working-memory challenge. NeuroImage Clinical. 2018; 19: 56-65.

43. Ghosh A, Rho Y, McIntosh AR, Kötter R, Jirsa VK. Noise during rest enables the exploration of the brain's dynamic repertoire. PLoS computational biology. 2008; 4 (10): e1000196.

44. Honey CJ, Sporns O, Cammoun L, et al. Predicting human resting-state functional connectivity from structural connectivity. Proceedings of the National Academy of Sciences of the United States of America. 2009; 106 (6): 2035-2040.

45. Zhang F, Daducci A, He Y, et al. Quantitative mapping of the brain's structural connectivity using diffusion MRI tractography: A review. NeuroImage. 2022; 249: 118870.

46. Hlinka J, Coombes S. Using computational models to relate structural and functional brain connectivity. The European journal of neuroscience. 2012; 36 (2): 2137-2145.

47. Ballotta D, Talami F, Pizza F, et al. Hypothalamus and amygdala functional connectivity at rest in narcolepsy type 1. NeuroImage Clinical. 2021; 31: 102748.

48. Sateia MJ. International Classification of Sleep Disorders-Third Edition. Chest. 2014; 146 (5): 1387-1394.

49. Dauvilliers Y, Jennum P, Plazzi G. Rapid eye movement sleep behavior disorder and rapid eye movement sleep without atonia in narcolepsy. Sleep medicine. 2013; 14 (8): 775-781.

50. Schenck CH, Mahowald MW. Motor dyscontrol in narcolepsy: rapid-eye-movement (REM) sleep without atonia and REM sleep behavior disorder. Annals of neurology. 1992; 32 (1): 3-10.

51. Mayer G, Kesper K, Ploch T, et al. Quantification of tonic and phasic muscle activity in REM sleep behavior disorder. Journal of clinical neurophysiology : official publication of the American Electroencephalographic Society. 2008; 25 (1): 48-55.

52. Nightingale S, Orgill JC, Ebrahim IO, de Lacy SF, Agrawal S, Williams AJ. The association between narcolepsy and REM behavior disorder (RBD). Sleep medicine. 2005; 6 (3): 253-258.

53. Nevsimalova S, Prihodova I, Kemlink D, Lin L, Mignot E. REM behavior disorder (RBD) can be one of the first symptoms of childhood narcolepsy. Sleep medicine. 2007; 8 (7-8): 784-786.

54. Knudsen S, Gammeltoft S, Jennum PJ. Rapid eye movement sleep behaviour disorder in patients with narcolepsy is associated with hypocretin-1 deficiency. Brain : a journal of neurology. 2010; 133 (Pt 2): 568-579.

55. Shen Y, Yu WB, Shen B, et al. Propagated α-synucleinopathy recapitulates REM sleep behaviour disorder followed by parkinsonian phenotypes in mice. Brain : a journal of neurology. 2020; 143 (11): 3374-3392.

56. Valencia Garcia S, Libourel PA, Lazarus M, Grassi D, Luppi PH, Fort P. Genetic inactivation of glutamate neurons in the rat sublaterodorsal tegmental nucleus recapitulates REM sleep behaviour disorder. Brain : a journal of neurology. 2017; 140 (2): 414-428.

57. Stiasny-Kolster K, Clever SC, Möller JC, Oertel WH, Mayer G. Olfactory dysfunction in patients with narcolepsy with and without REM sleep behaviour disorder. Brain : a journal of neurology. 2007; 130 (Pt 2): 442-449.

58. Jiménez-Jiménez FJ, Alonso-Navarro H, García-Martín E, Agúndez JAG. Neurochemical Features of Rem Sleep Behaviour Disorder. Journal of personalized medicine. 2021; 11 (9).

59. Nishino S, Ripley B, Overeem S, Lammers GJ, Mignot E. Hypocretin (orexin) deficiency in human narcolepsy. Lancet (London, England). 2000; 355 (9197): 39-40.

60. Schöne C, Burdakov D. Glutamate and GABA as rapid effectors of hypothalamic "peptidergic" neurons. Frontiers in behavioral neuroscience. 2012; 6: 81.

61. Schöne C, Apergis-Schoute J, Sakurai T, Adamantidis A, Burdakov D. Coreleased orexin and glutamate evoke nonredundant spike outputs and computations in histamine neurons. Cell reports. 2014; 7 (3): 697-704.

62. Plaza-Zabala A, Li X, Milovanovic M, et al. An investigation of interactions between hypocretin/orexin signaling and glutamate receptor surface expression in the rat nucleus accumbens under basal conditions and after cocaine exposure. Neuroscience Letters. 2013; 557: 101-106.

63. Acuna-Goycolea C, Li Y, Van Den Pol AN. Group III metabotropic glutamate receptors maintain tonic inhibition of excitatory synaptic input to hypocretin/orexin neurons. The Journal of neuroscience : the official journal of the Society for Neuroscience. 2004; 24 (12): 3013-3022.

64. Chang MC, Park JM, Pelkey KA, et al. Narp regulates homeostatic scaling of excitatory synapses on parvalbumin-expressing interneurons. Nature neuroscience. 2010; 13 (9): 1090-1097.

65. Reti IM, Reddy R, Worley PF, Baraban JM. Selective expression of Narp, a secreted neuronal pentraxin, in orexin neurons. Journal of neurochemistry. 2002; 82 (6): 1561-1565.

66. Alakurtti K, Johansson JJ, Joutsa J, et al. Long-term test–retest reliability of striatal and extrastriatal dopamine D2/3 receptor binding: study with [11C] raclopride and high-resolution PET. 2015; 35 (7): 1199-1205.

Figure Legend

Figure 1 Topology features of structural network in patients with narcolepsy (**A**) An overview for building the contrast matrix. (**B**) The narcolepsy featured contrast matrix. (**C**) Group comparison of Graph-Theory features in the global structural network of narcolepsy patients and matched HCs as well as subgroups of narcolepsy patients ($^{***}P < 0.001$). (**D**) The *t*-value distribution in regional topological features (nodal degree and nodal efficiency) of the narcolepsy patients, where the dashed line represents the *t*-value threshold after FDR correction. (**E**) Network-based statistics revealed a subnetwork of hyperenhanced connectivity strength in the narcolepsy patients. **(F)** Group comparison of Graph-Theory features in the RBD-sensitive subnetwork of narcolepsy patients and matched HCs as well as subgroups of narcolepsy patients ($^{***}P < 0.001$, $^{*}P < 0.05$).

Figure 2 Linking structural topology to clinical characteristics of narcolepsy patients Correlation results between metrics of global structural network of narcolepsy patients and MSLT sleep latency (**A**), sleep latency at PSG (**A**), wake time after sleep onset (**B**), awakening number per hour (**B**), N1 sleep time and percentage (**C**) and N2 sleep time and percentage (**D**).

Figure 3 Linking structural narcolepsy topology to glutamatergic neuropathophysiology (**A**) Significant results of Panther pathway terms in the functional enrichment analysis performed by WebGestalt. (**B**) Bar graph of GO enrichment analysis based on affinity propagation for narcolepsy-featured genes. (**C**) Further verification by glutamatergic PET/SPECT data.

Table

Table 1 Characteristics of the study population

	Patients (n = 30)	**Matched HCs (n = 30)**	***P* value**
Basic information			
Male: Female	18:12	18:12	*P > 0.05*
Age (years, mean, SD)	29.5 (13.5)	29 (12.8)	*P > 0.05*
Narcolepsy features			
EDS (n/total)	30/30	0/30	*P < 0.001*
EDS duration (years, mean, SD)	10.0 (7.0)	-	-
Cataplexy (n/total)	17/30	0/30	*P < 0.001*
Sleep paralysis (n/total)	6/30	0/30	*P < 0.001*
Hypnagogic hallucinations (n/total)	12/30	0/30	*P < 0.001*
RBD (n/total)	19/30	0/30	*P < 0.001*
Narcolepsy testing			
ESS score (mean, SD)	15.4 (5.2)	2.8 (2.0)	*P < 0.001*
MSLT sleep latency (minutes, mean, SD)	2.25 (1.39)	-	-
Night polysomnography			
TST (minutes, mean, SD)	411.7 (53.4)	-	-
Sleep latency (minutes, mean, SD)	9.0 (8.7)	-	-
Sleep efficiency (minutes, mean, SD)	85.6 (10.6)	-	-
N1 Sleep (% of TST, mean, SD)	29.3 (10.3)	-	-
N2 Sleep (% of TST, mean, SD)	39.5 (12.6)	-	-
N3 Sleep (% of TST, mean, SD)	13.8 (6.4)	-	-
REM Sleep (% of TST, mean, SD)	17.5 (6.2)	-	-

REM times (mean, SD)	4.6 (1.3)	-	-
REM latency (minutes, mean, SD)	92.8 (74.5)	-	-
Wake time after sleep onset (WASO)	26.5 (24)	-	-
Awakening number (AWN) per hour (mean, SD)	4.0 (3.4)		
Micro-arousal index (MAI) (mean, SD)	3.8 (5.7)	-	-
Oxygen desaturation index (ODI) (mean, SD)	5.0 (6.0)	-	-
Limb movement (LM) index (mean, SD)	22.1 (18.6)	-	-
Periodic leg movements (PLM) index (mean, SD)	9.1 (16.9)	-	-

Note: HC: health control; MSLT: multiple sleep latency test; ESS: Epworth Sleepiness Scale; RBD: rapid eye movement (REM) sleep behavior disorder; EDS: excessive daytime sleepiness

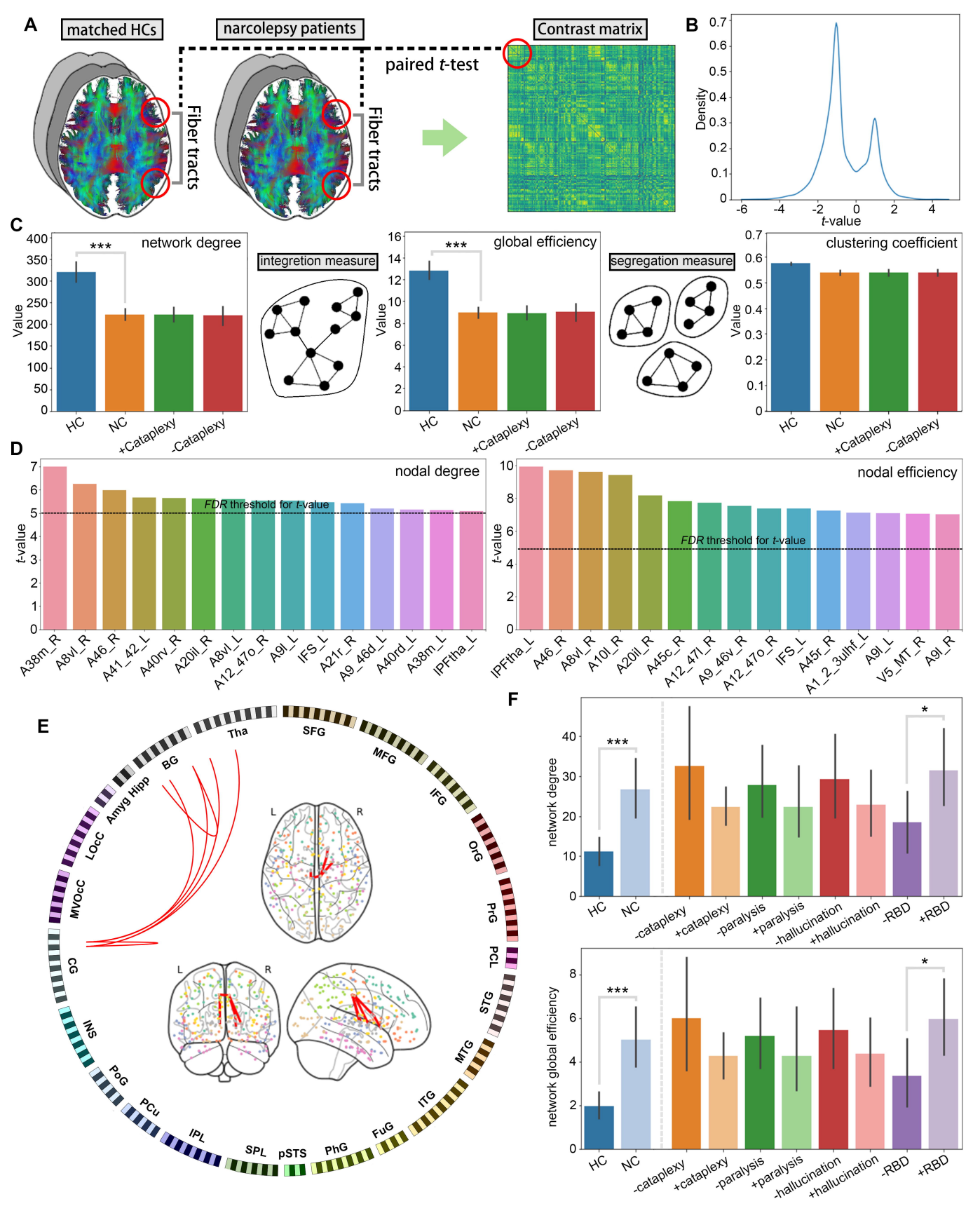
A
matched HCs
narcolepsy patients
Contrast matrix
paired t-test
Fiber tracts
Fiber tracts
B
Density
t-value
C
network degree
***
Value
HC
NC
+Cataplexy
-Cataplexy
integretion measure
global efficiency
segregation measure
clustering coefficient
D
nodal degree
FDR threshold for t-value
t-value
A38m_R
A8vl_R
A46_R
A41_42_L
A40rv_R
A20il_R
A8vl_L
A12_47o_R
A9l_L
IFS_L
A21r_R
A9_46d_L
A40rd_L
A38m_L
IPFtha_L
nodal efficiency
IPFtha_L
A46_R
A8vl_R
A10l_R
A20il_R
A45c_R
A12_47l_R
A9_46v_R
A12_47o_R
IFS_L
A45r_R
A1_2_3ulhf_L
A9l_L
V5_MT_R
A9l_R
E
Tha
SFG
MFG
IFG
OrG
PrG
PCL
STG
MTG
ITG
FuG
PhG
pSTS
SPL
IPL
PCu
PoG
INS
CG
MVOcC
LOcC
Amyg Hipp
BG
L
R
F
network degree
network global efficiency
*
HC
NC
-cataplexy
+cataplexy
-paralysis
+paralysis
-hallucination
+hallucination
-RBD
+RBD

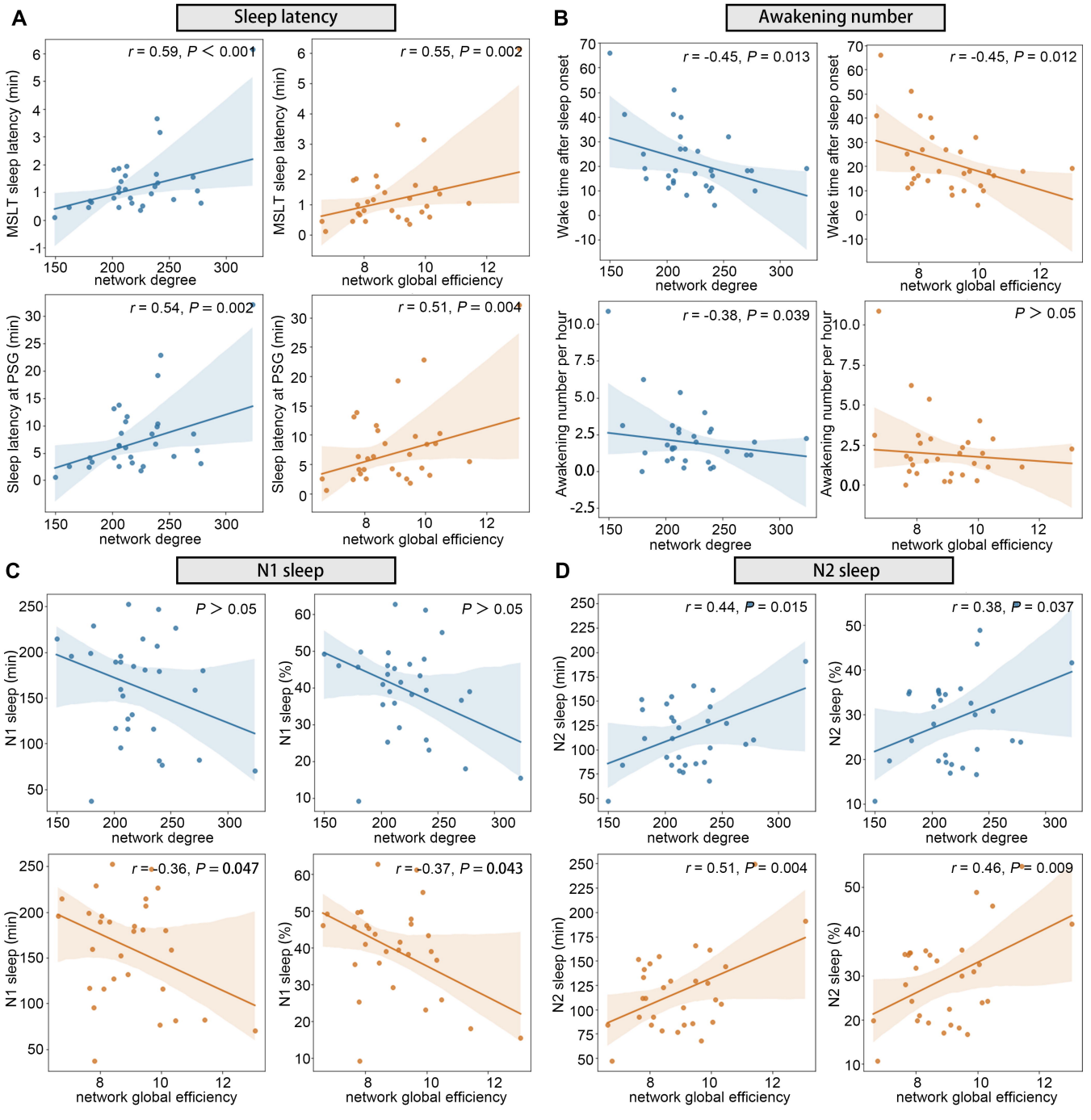
A
Sleep latency
r = 0.59, P < 0.001
MSLT sleep latency (min)
network degree
r = 0.55, P = 0.002
MSLT sleep latency (min)
network global efficiency
r = 0.54, P = 0.002
Sleep latency at PSG (min)
network degree
r = 0.51, P = 0.004
Sleep latency at PSG (min)
network global efficiency
B
Awakening number
r = -0.45, P = 0.013
Wake time after sleep onset
network degree
r = -0.45, P = 0.012
Wake time after sleep onset
network global efficiency
r = -0.38, P = 0.039
Awakening number per hour
network degree
P > 0.05
Awakening number per hour
network global efficiency
C
N1 sleep
P > 0.05
N1 sleep (min)
network degree
P > 0.05
N1 sleep (%)
network degree
r = -0.36, P = 0.047
N1 sleep (min)
network global efficiency
r = -0.37, P = 0.043
N1 sleep (%)
network global efficiency
D
N2 sleep
r = 0.44, P = 0.015
N2 sleep (min)
network degree
r = 0.38, P = 0.037
N2 sleep (%)
network degree
r = 0.51, P = 0.004
N2 sleep (min)
network global efficiency
r = 0.46, P = 0.009
N2 sleep (%)
network global efficiency

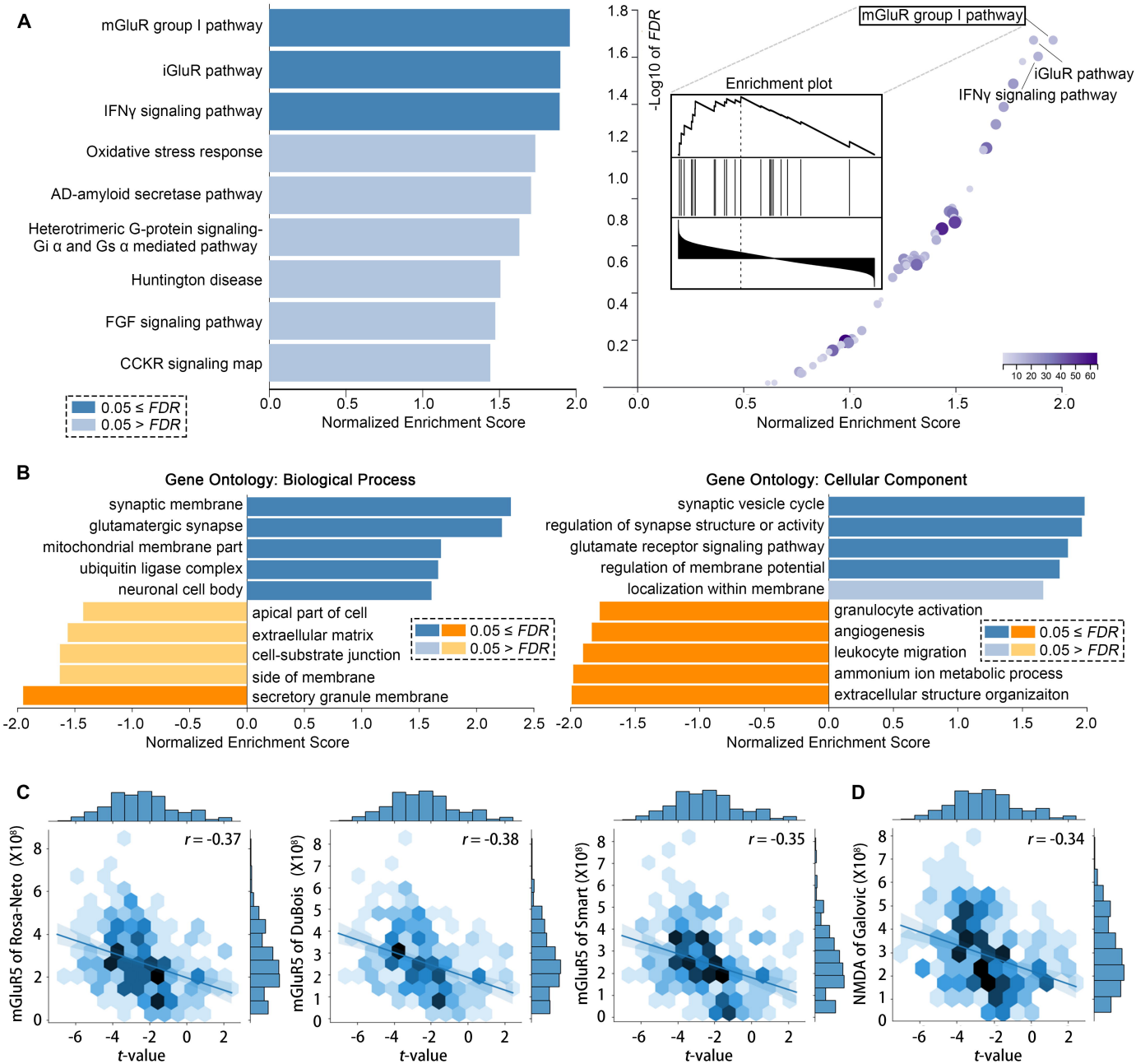
A
mGluR group I pathway
iGluR pathway
IFNγ signaling pathway
Oxidative stress response
AD-amyloid secretase pathway
Heterotrimeric G-protein signaling-Gi α and Gs α mediated pathway
Huntington disease
FGF signaling pathway
CCKR signaling map
0.05 ≤ FDR
0.05 > FDR
Normalized Enrichment Score
-Log10 of FDR
Enrichment plot
mGluR group I pathway
iGluR pathway
IFNγ signaling pathway
B
Gene Ontology: Biological Process
synaptic membrane
glutamatergic synapse
mitochondrial membrane part
ubiquitin ligase complex
neuronal cell body
apical part of cell
extraellular matrix
cell-substrate junction
side of membrane
secretory granule membrane
Gene Ontology: Cellular Component
synaptic vesicle cycle
regulation of synapse structure or activity
glutamate receptor signaling pathway
regulation of membrane potential
localization within membrane
granulocyte activation
angiogenesis
leukocyte migration
ammonium ion metabolic process
extracellular structure organizaiton
C
D
r = -0.37
r = -0.38
r = -0.35
r = -0.34
mGluR5 of Rosa-Neto (X10⁸)
mGluR5 of DuBois (X10⁸)
mGluR5 of Smart (X10⁸)
NMDA of Galovic (X10⁸)
t-value